

# Properties of $I_A$ in a serotonergic neuron of the dorsal raphe nucleus

Nicholas J. Penington<sup>1,2</sup>, Henry C. Tuckwell<sup>3†</sup>

<sup>1</sup> Department of Physiology and Pharmacology,

<sup>2</sup> Program in Neural and Behavioral Science and Robert F. Furchgott Center  
for Neural and Behavioral Science

State University of New York, Downstate Medical Center,  
Box 29, 450 Clarkson Avenue, Brooklyn, NY 11203-2098, USA

<sup>3</sup> Max Planck Institute for Mathematics in the Sciences  
Inselstr. 22, 04103 Leipzig, Germany

<sup>†</sup> *Corresponding author:* tuckwell@mis.mpg.de

February 12, 2022

*Abbreviated title:* Estimation of activation function for  $I_A$  in DRN

## Abstract

Voltage clamp data were analyzed in order to characterize the properties of the fast potassium transient current  $I_A$  for a serotonergic neuron of the rat dorsal raphe nucleus (DRN). We obtain maximal conductance, time constants of activation and inactivation, and the steady state activation and inactivation functions  $m_\infty$  and  $h_\infty$ , as Boltzmann curves, defined by half-activation potentials and slope factors. We employ a novel method to accurately obtain the activation function and compare the results with those obtained by other methods. The form of  $I_A$  is estimated as  $\bar{g}(V - V_{rev})m^4h$ , with  $\bar{g} = 20.5$  nS. For activation, the half-activation potential is  $V_a = -52.5$  mV with slope factor  $k_a = 16.5$  mV, whereas for inactivation the corresponding quantities are -91.5 mV and -9.3 mV. We discuss the results in terms of the corresponding properties of  $I_A$  in other cell types and their possible relevance to pacemaking activity in 5-HT cells of the DRN.

Keywords: Serotonin; dorsal raphe nucleus; potassium transient current; activation.

# 1 Introduction

Serotonergic neurons in the DRN, which extensively innervate most brain regions, have a large influence on many aspects of behavior, including sleep-wake cycles, mood and impulsivity (Liu et al, 2004; Miyazaki et al., 2011). The firing patterns of these cells have been much studied and many properties of the ionic currents underlying action potentials have been investigated (Aghajanian, 1985; Segal, 1985; Burlhis and Aghajanian, 1987; Penington et al., 1991, 1992; Penington and Fox, 1995). In order to quantitatively analyze action potential generation in DRN 5-HT neurons, it is desirable to have accurate knowledge of the activation and inactivation properties of the various ion currents for some of which there is relatively little or no data available. Here we report results for the fast transient potassium current  $I_A$  which plays an important role in determining the cell's firing rate.

Mathematical modeling of electrophysiological dynamics has been pursued for many different nerve and muscle cell types. Some well known neuronal examples are thalamic relay cells (Huguenard and McCormick, 1992; Destexhe et al., 1998; Rhodes and Llinas, 2005), dopaminergic cells (Komendantov et al., 2004; Putzier et al., 2009; Kuznetsova et al., 2010), hippocampal pyramidal cells (Traub et al., 1991; Migliore et al., 1995; Poirazi et al., 2003; Xu and Clancy, 2008) and neocortical pyramidal cells (Destexhe et al., 2001; Traub et al, 2003; Yu et al., 2008). Cardiac myocytes have also been the subject of numerous computational modeling studies with similar structure and equivalent complexity to that of neurons (Faber et al., 2007; Williams et al., 2010).

The methods employed by Hodgkin and Huxley (1952) to describe mathematically the time (and space) course of nerve membrane potential have, for the most part, endured to the present day. An integral component of their model consists of differential equations for activation and (if present) inactivation variables, generically represented in the non-spatial models as  $m(t, V)$  and  $h(t, V)$ , respectively, where  $t$  is time and  $V$  is membrane potential. These equations are

$$\frac{dm}{dt} = \frac{m_\infty - m}{\tau_m}, \quad \frac{dh}{dt} = \frac{h_\infty - h}{\tau_h}, \quad (1)$$

where  $m_\infty(V)$  and  $h_\infty(V)$  are steady state values and  $\tau_m$  and  $\tau_h$  are time constants which often depend on  $V$ . For voltage-gated ion channels the current is often assumed to be

$$I = \bar{g}(V - V_{rev})m^ph \quad (2)$$

where  $\bar{g}$  is the maximal conductance,  $V_{rev}$  is the reversal potential for the ion species under consideration and  $p$  is (usually) a small non-negative integer between 1 and 4. The inactivation is invariably to the power one, as in (2). Although these equations have solutions which can only yield approximations to actual currents, it is nevertheless desirable to have accurate forms for the steady state activation and inactivation functions  $m_\infty(V)$  and  $h_\infty(V)$ , the time constants  $\tau_m(V)$  and  $\tau_h(V)$ , and the remaining parameters  $\bar{g}$  and  $V_{rev}$ . Our concern in this article is to describe and illustrate a novel and straightforward yet accurate method of estimating these quantities from voltage-clamp data.

## 2 Results

In order to isolate  $I_A$ , currents for activation and inactivation protocols were obtained in 20 mM TEA, as described in Section 4.1, for several identified serotonergic neurons of the rat dorsal raphe nucleus. In many cells the outward currents were clearly a mixture of components with different dynamical properties. In some cells, however, the currents decayed smoothly from an early peak to near zero and were apparently a manifestation of a single channel type, presumed to be uncontaminated  $I_A$ . Thus neither  $\text{CoCl}_2$  nor  $\text{CdCl}_2$  was employed. One cell in particular, DR5, with an apparently pure set of current traces was singled out for analysis. Its activation current traces are shown in Figure 1. Results for other cells with composite outward currents will be analyzed in future articles.



Figure 1: Activation current traces under voltage clamp for cell DR5 in 20 mM TEA. Time marker, 100 ms, Current marker, 100 pA. Voltage stepped from -120 mV to -60, -50, -40, -30 and -20 mV. For experimental protocol see Section 4.1.

The current traces of Figure 1 were obtained in digitized form and the time constants  $\tau_m$  and  $\tau_h$  and the value of  $p$  were estimated by the best fitting of the current traces to the analytical formula (6). Only two of these three parameters can be independently chosen by virtue of the constraint given by formula (7)

for the time of occurrence  $t_{max}$  of the maximum current, which rearranges to

$$\tau_h = \frac{\tau_m}{p} \left( e^{\frac{t_{max}}{\tau_m} - 1} \right) \quad (3)$$

The current was required to pass through the maximum point at  $(t_{max}, I_{max})$  and one other point on the trace, called  $(t_2, I_2)$ . The value of  $p = 4$  was found to give excellent fits to the current traces. An example of the resulting curve with best fitting time constants  $\tau_m$  and  $\tau_h$  is shown in Figure 2 along with the experimental current for a step from -120 mV to -20 mV.

Table 1 summarizes the data and estimates of time constants for cell DR5, all of which quantities are required to estimate the three parameters  $\bar{g}$  (conductance),  $V_a$  and  $k_a$  (Boltzmann parameters for activation). In this table  $I_{A,max}$  is the maximal experimental current over time.

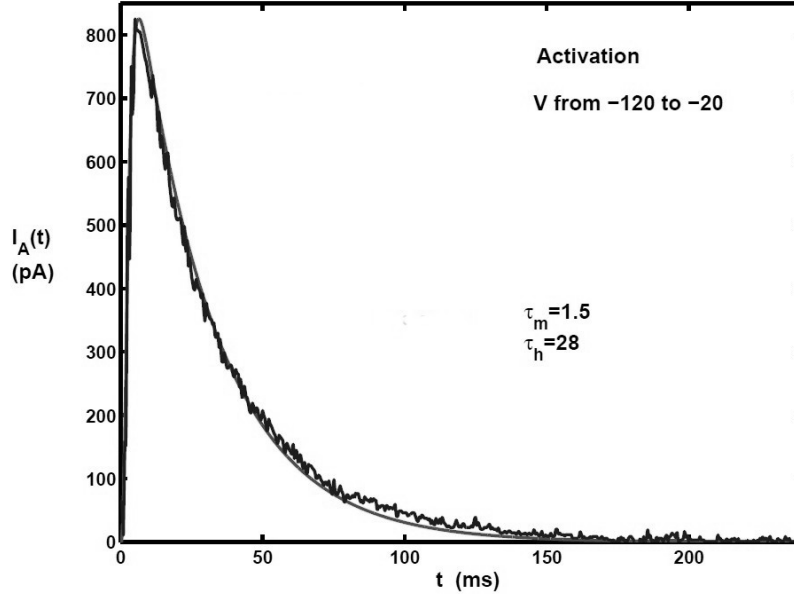


Figure 2: An example of the best fitting curve for the calculated time-dependent current  $I_A(t)$  (smooth curve), as given in Equation (6) with  $p = 4$ , to an experimental trace for cell DR5 with calculated time constants for activation  $\tau_m = 1.5$  ms, and inactivation  $\tau_h = 28$  ms. Voltage stepped from -120 mV to -20 mV.

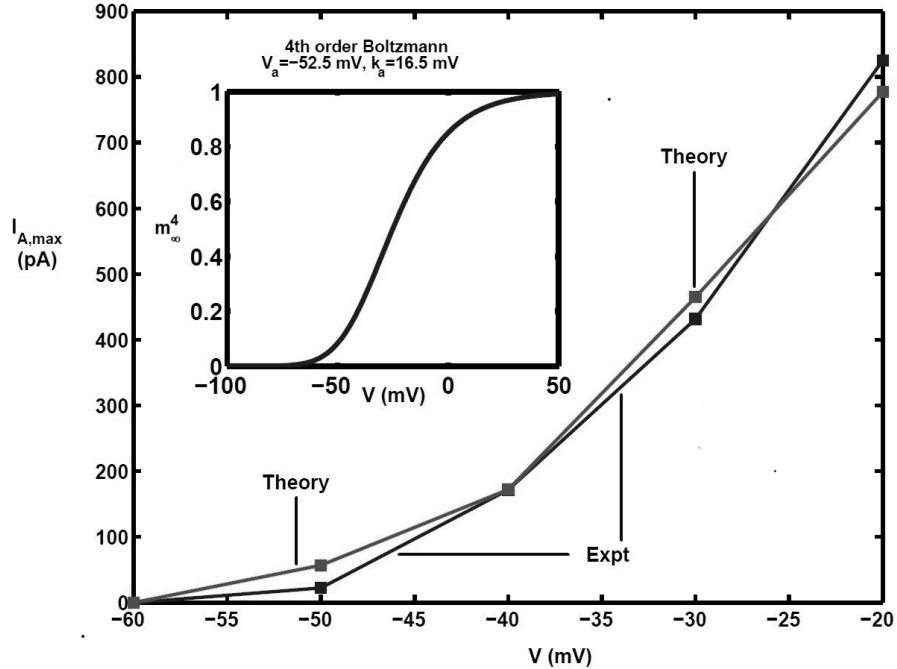
The results obtained by nonlinear least-squares fitting (Section 4.2.2) with correction factor as in Equation (8) and following but without making any assumption about  $V^*$ , (called method A), are that for cell DR5 the whole cell maximal conductance for the  $I_A$  channels is  $\bar{g} = 20.5$  nS, the half-activation

Table 1: Maximal currents and estimated time constants in activation experiments for  $I_A$  in cell DR5

Step from -120 mV to	$I_{A,max}$ (pA)	$\tau_m$ (ms)	$\tau_h$ (ms)
-20 mV	825.4	1.5	28.0
-30 mV	431.7	1.5	28.0
-40 mV	171.5	2.4	21.7
-50 mV	22.2	-	-
-60 mV	0	-	-

potential is  $V_a = -52.5$  mV and the corresponding slope factor is  $k_a = 16.5$  mV (see also Table 2).

As a check on the estimated parameter values by method A, the maximal currents with steps from  $V_0 = -120$  mV to  $V_1 = -60, -50, -40, -30$  and  $-20$  mV were calculated by formula (8) using the values  $\bar{g} = 20.5$  nS,  $V_a = -52.5$  mV,  $k_a = 16.5$  mV,  $p = 4$ ,  $V_{rev} = -105$  mV and the time constants given in Table 1. The maximal currents so determined are plotted against  $V_1$  in Figure 3 where it can be seen that there is excellent agreement with the experimental values. Also shown in the inset of the Figure is the activation function raised to the power 4, a so called 4th order Boltzmann.



It is interesting to compare the values of the activation function so obtained

Figure 3: Predicted and experimental values of  $I_{max}$  in activation protocols stepped up from -120 mV to various clamp voltages, in mV, -60, -50, -40, -30 and -20, for cell DR5 with TEA 20 mM. The inset shows the best fitting 4th order Boltzmann.

with those obtained by three other procedures. For method B, in which it is assumed that  $V^* = -20$  mV so that  $m_\infty(-20) = 1$  (see note after Equation (11)), which implies that Equation (12) gives an estimate of  $\bar{g}$ , the values  $\bar{g} = 12.91$  nS,  $V_a = -54.7$  mV and  $k_a = 12.52$  mV are obtained.

In method C, the value of  $V^*$  is not fixed but a best-fitting Boltzmann is obtained by least squares, which gives  $V_a = -47.0$  mV and  $k_a = 10.2$  mV. It is also of interest to compare these sets of results with those by the usual method, called method D, using the raw  $G/G_{max}$  values which assumes that  $V^* = -20$  mV. This gives  $V_a = -48.2$  mV and  $k_a = 11.78$  mV.

It can be seen from the data in Table 2 that there are considerable discrepancies between the results obtained by the various methods. Method A gives the most accurate estimates. For the other three methods, relative errors in the conductance are between -37.1 % and -52.6 % relative errors in  $V_a$  are from -10.5 % to +4.2 % and those in  $k_a$  are from -24.1 % to -38.2 %. Such errors can clearly lead to significant errors in the computed ionic currents.

Table 2: Estimated activation function and conductance of  $I_A$  for cell DR5, obtained by four methods as described in the text: % errors relative to method A given in brackets

Method →	A	B	C	D
$\bar{g}$ (nS)	20.5	12.9 (-37.1)	12.4 (-39.5)	9.71 (-52.6)
$V_a$ (mV)	-52.5	-54.7 (+4.2)	-47 (-10.5)	-48.2 (-8.2)
$k_a$ (mV)	16.5	12.52 (-24.1)	10.2 (-38.2)	11.78 (-28.6)

## 2.1 Inactivation experiments

For the inactivation voltage-clamp experiments, whose results are not shown, the maximum currents  $I_{max}(V_0, V_1)$  at various starting potentials  $V_0$  are sufficient to estimate the relative values of the inactivation function because all factors on the right hand side of (17) except  $h_\infty(V_0)$  do not depend on  $V_0$ . Assuming that  $h_\infty(-120) = 1$ , the best fitting steady state inactivation function was

$$h_\infty(V) = \frac{1}{1 + e^{(V+91.5)/9.3}}. \quad (4)$$

## 2.2 Graphical summary

The activation functions obtained by methods A-D and the inactivation function for the transient potassium current  $I_A$  in cell DR5 are drawn in the top panel of

Figure 4. Also shown, in the lower panel, is the activation function to power 4, which reflects more closely the contribution of activation to current amplitudes at various membrane potentials.

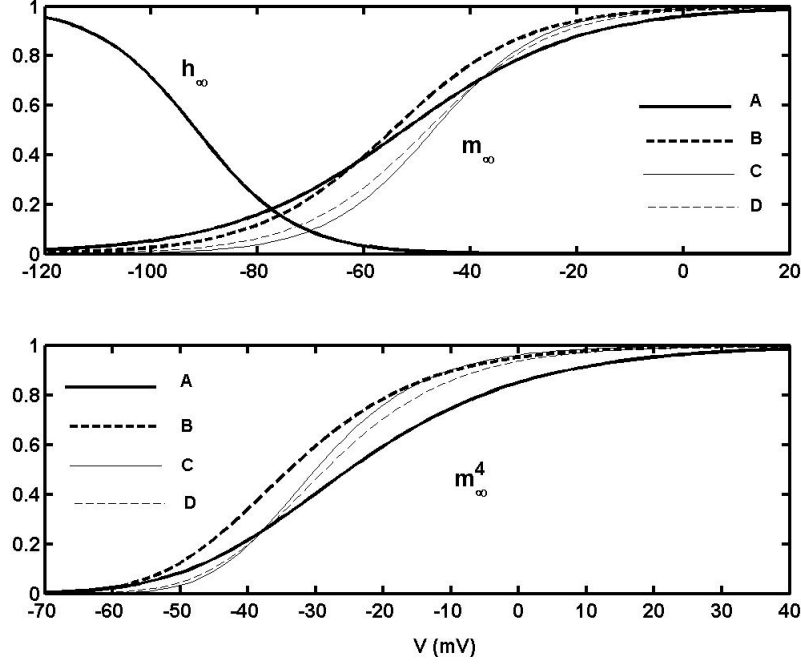


Figure 4: *Top part.* Steady state inactivation function and steady state activation function obtained by the methods A-D as explained in the text for  $I_A$  in cell DR5 obtained from voltage-clamp data by the methods described. The result for method A is the most accurate estimate of  $m_\infty$ . *Lower part.* The activation function to the power 4 is shown for the methods A-D.

### 3 Discussion

There have been many investigations of the properties of the ionic currents involved in the firing of serotonergic neurons of the dorsal raphe nucleus (Aghajanian, 1985; Segal, 1985; Burlhis and Aghajanian, 1987; Penington et al., 1991, 1992; Penington and Fox, 1995; Chen et al., 2002). However, the basis of apparent pacemaker-like activity in these cells is not fully understood. It was claimed that noradrenergic input is required (Burlhis and Aghajanian, 1987) for firing in some cells and there have been conflicting ideas about the role of  $I_A$  (Burlhis and Aghajanian, 1987; Segal, 1985). No reports on the properties of  $I_A$  in these cells have previously appeared.

In the first quantitative study of  $I_A$ , Connor and Stevens (1971) reported an  $m^4h$  form for the current in a single gastropod neuron and found quite long time constants for activation (12 ms) and inactivation (235 ms). The  $V_{1/2}$  value for inactivation was -68 mV, with a resting potential of -40 mV. It was also found that  $I_A$  was important mainly in the middle and end of the interspike interval (ISI, see below). Concerning the method of analyzing voltage-clamp data for activation, in their pioneering work on squid axon, for large depolarizations Hodgkin and Huxley (1952) used the general Equation (5) for the time-dependent sodium current converted to a conductance

$$g(t) = \bar{g}[m_\infty(V_1)(1 - e^{-t/\tau_m})]^3 h_\infty(V_0)e^{-t/\tau_h}$$

to estimate  $\bar{g}[m_\infty(V_1)]^3 h_\infty(V_0)$ . Belluzzi and Sacchi (1988) also employed Equation (5) with simplifying assumptions for  $m$  and  $h$ , and  $p$  as a parameter. Activation time constants were estimated via Equation (7) with  $p = 3$ , the small values of both  $\tau_m$  and  $\tau_h$  they obtained reflecting the relatively high temperature of the preparation. For activation in histamine neurons, Greene et al. (1990) found a fast and slow component of  $I_A$  and reported Boltzmann parameters for normalized current without converting to conductances. Huguenard and McCormick (1992) used normalized currents to find inactivation parameters and time-courses of conductances (as in (5)) to determine Boltzmann parameters for activation. Bekkers (2000) gave two sets of results for activation, one obtained from the empirical Boltzmann fit to the peak  $I_A$  conductance curve, and the other obtained from the time-dependent  $I_A$  conductance curves. We have pursued a new approach, as outlined in the last section, which utilizes the maxima of the currents at various clamp voltages and employed a correction factor as in Equation (8).

The results obtained for  $I_A$  in a serotonergic cell of rat DRN are compared with those in some other CNS preparations in Table 3. It can be seen that the half-activation potentials for activation are generally similar and that the largest variation occurs in the time constant of inactivation.

In order to construct a computational model of action potential generation in DRN 5-HT neurons, such that the role of the various ionic components can be properly understood, it is desirable to have accurate knowledge of the activation and inactivation properties of the various ion currents, including that addressed here,  $I_A$ . The need for considerable accuracy is made the more important because several components, including the low threshold T-type calcium and  $I_A$  operate in overlapping ranges of potential. In this paper we have illustrated that the often-used procedure of finding activation functions  $m_\infty(V_1)$  by taking ratios of current to maximal current or conductance to maximal conductance may produce inaccurate results due to the fact that the quantity  $F_p(\gamma)$  in (8) depends on the clamp voltage and does not cancel. Not taking this into account can lead to substantial errors in the estimates of the parameters  $k_a$  and  $V_a$ . Inactivation functions, however, do not have such a complication and can be estimated in the usual way.



Table 3: Activation and inactivation parameters for  $I_A$  in some CNS cells

	DRN serotonergic <sup>a</sup>	Sympathetic cervical ganglion <sup>b</sup>	Thalamic relay <sup>c</sup>	Cortical pyramid <sup>d</sup>
Activation				
$V_{1/2}$ mV	-52.5	-58.55	-60	-56.2
$k$ mV	16.5	14.39	8.5	19.1
$\tau_m$ ms	1.5-2.4	< 1	0.5-2.5	0.3-8
Inactivation				
$V_{1/2}$ mV	-91.5	-78	-78	-81.6
$k$ mV	9.3	7.3	6	6.7
$\tau_h$ ms	21.7-28.0	< 10	12-65	6-8

<sup>a</sup>This study; <sup>b</sup>Belluzzi & Sacchi (1988); <sup>c</sup>Huguenard & McCormick (1992);

<sup>d</sup>Bekkers (2000).

L-type calcium currents, particularly through  $Ca_v1.3$  channels, have been found to sometimes play a role in pacemaker activity in neurons and cardiac cells (Koschak et al., 2003; Putzier et al., 2009; Marcantoni et al., 2010). However, in DRN 5-HT cells, there is only a small (about 4% of total  $I_{Ca}$ ) contribution from L-type calcium currents (Penington et al., 1991) so it is yet to be determined what role these play in the pacemaking activity. These latter results were, however, obtained in dissociated cells. Burlhis and Aghajanian (1987) hypothesized that the low threshold calcium T-type current played a key role in pacemaking and Segal (1985) proposed that  $I_A$  was also important. However, considering the fact that the resting potential for these cells is about -60 mV and that threshold for spiking is about -50 mV, and judging by the curves for  $m_\infty(V)$  and  $h_\infty(V)$  in Figure 4, it is likely that  $I_A$  is only important during the spike itself and not between the commencement of the afterhyperpolarization and the next spike, probably implying a lesser role for  $I_A$  in pacemaking as it tends to be switched off during the greater part of the ISI. We will explore by means of a computational model the ionic basis of the mechanisms of pacemaking in DRN 5-HT cells in future articles.

Finally we note that the  $I_A$  results obtained here for  $m_\infty$  and the time constants bear a resemblance to those given in Gutman et al. (2005) for the transient A-type channels  $K_v4.1$  ( $V_a = -47.9$  mV,  $k_a = 24$  mV,  $\tau_h = 22$  ms, and two other  $\tau_h$  values). This contrasts with the finding by Bekkers (2000) who suggested that in rat layer 5 cortical pyramidal cells,  $I_A$  was carried by  $K_v4.2$  channels, which accounts for their smaller time constants of inactivation (Gutman et al., 2005).

## 4 Materials and Methods

### 4.1 Experimental

Data of the kind analyzed in this paper were obtained from 2 month-old male Sprague-Dawley rats that were anesthetized with halothane and then decapitated with a small animal guillotine in accordance with our local Animal Care and Use Committee regulations. Three coronal slices (500  $\mu\text{m}$ ) through the brain stem at the level of the DRN were prepared using a vibroslice in a manner that has previously been described (Yao et al., 2010). Pieces of tissue containing the DRN were then incubated in a PIPES buffer solution containing 0.2 mg/mL trypsin (Sigma Type XI) under pure oxygen for 120 min. The tissue was then triturated in Dulbecco's modified Eagle's medium to yield individual neuronal cell bodies with vestigial processes. Recording was carried out at room temperature, 20°C-25°C. Cells recorded from had diameters of about 20  $\mu\text{m}$ . Steinbusch et al. (1981) showed using immunohistochemistry that most of the cells in a thin raphe slice with a soma diameter greater than 20  $\mu\text{m}$  contain 5-HT while the smaller cells were largely GABAergic interneurons. Using a method similar to that of Yamamoto et al. (1981), we also found that the proportion of isolated cells with diameters larger than 20  $\mu\text{m}$  that stain for 5-HT, was greater than 85%, and a similar percentage responded to serotonin.

The cells were voltage-clamped using a switching voltage clamp amplifier (Axoclamp 2A) and a single patch pipette in the whole-cell configuration (Hamill et al., 1981). Pipettes pulled from thick-walled borosilicate glass (resistance from 5-7 M $\Omega$ ) allowed a switching frequency of 8-13 KHz with a 30% duty cycle. The seal resistance measured by the voltage response to a 50 pA step of current was often greater than 5 G $\Omega$ ). The voltage-clamp data were filtered at 1 KHz and digitized for storage at 16 bits, or experiments were run online with a PC and a CED 1401 interface.

The external saline was designed to isolate potassium currents and contained: outside the cell TTX 0.2  $\mu\text{M}$  and in mM NaCl 147, KCl 2.5, CaCl<sub>2</sub> 2, MgCl<sub>2</sub> 2, Glucose 10, HEPES 20, pH 7.3. Inside: K<sup>+</sup> Gluconate 84, MgATP 2, KCl 38, EGTA-KOH 11, HEPES 10, CaCl<sub>2</sub> 1, pH 7.3. The total [K<sup>+</sup>] inside was 155mM (since 33 mM is added to make the salt of EGTA). The osmolarity was adjusted with sucrose so that the pipette solution was 10 mOsm hypoosmotic to the bath solution. Drugs were either dissolved in the extracellular solution and added to the perfusate or applied by diffusion from a patch pipette (tip 15  $\mu\text{m}$ ) lowered close to the cell (50  $\mu\text{m}$  and then removed from the bath). As a control, the same procedure was carried out without addition of the drug to the application pipette; this did not affect  $I_A$ . In some cells, to investigate any influence of Ca<sup>2+</sup> currents on  $I_A$  either 2 mM CoCl<sub>2</sub> or 20  $\mu\text{M}$  CdCl<sub>2</sub> was added to the bath by a pipette placed near the cell. This sometimes changed the magnitude of  $I_A$  but had little effect on its time course.

## 4.2 Theory

Suppose that in a voltage clamp experiment the voltage is, after equilibration at a voltage  $V_0$ , suddenly clamped at the new voltage  $V_1$ . Then, assuming a current of the form of Equation (2), according to the standard Hodgkin-Huxley (1952) theory, the current at time  $t$  after the switch to  $V_1$  is

$$I(t; V_0, V_1) = \bar{g}(V_1 - V_{rev})[m_1 - (m_1 - m_0)e^{-t/\tau_m}]^p[h_1 - (h_1 - h_0)e^{-t/\tau_h}], \quad (5)$$

where we have employed the abbreviations  $m_0 = m_\infty(V_0)$ ,  $m_1 = m_\infty(V_1)$  for the activation,  $h_0 = h_\infty(V_0)$ ,  $h_1 = h_\infty(V_1)$  for the inactivation and  $\tau_m = \tau_m(V_1)$ ,  $\tau_h = \tau_h(V_1)$  for the time constants.

### 4.2.1 Activation experiments

In activation experiments there is a step up from a relatively hyperpolarized state  $V_0$  to several more depolarized states  $V_1$  so that one usually assumes that  $h_0 = 1$ ,  $h_1 = 0$  and  $m_0 = 0$ . This gives the simplified expression for the current

$$I(t; V_1) = \bar{g}(V_1 - V_{rev})[m_\infty(V_1)(1 - e^{-t/\tau_m})]^p e^{-t/\tau_h}. \quad (6)$$

Finding the maximum by differentiation yields the time at which the maximum occurs as

$$t_{max}(V_1) = \tau_m \ln \left( 1 + \frac{p\tau_h}{\tau_m} \right) \quad (7)$$

and its value as

$$I_{max}(V_1) = \bar{g}(V_1 - V_{rev})m_\infty^p(V_1)F_p(\gamma) \quad (8)$$

where

$$F_p(\gamma) = \frac{(p\gamma)^p}{(1 + p\gamma)^{p+1/\gamma}} \quad (9)$$

and where  $\gamma$ , which depends on  $V_1$ , is defined as

$$\gamma(V_1) = \frac{\tau_h(V_1)}{\tau_m(V_1)}. \quad (10)$$

Since  $V_1$  is here considered a variable, the time course of the current changes as  $V_1$  varies. By rearrangement the steady state activation is given by

$$m_\infty(V_1) = \left( \frac{I_{max}(V_1)}{\bar{g}(V_1 - V_{rev})F_p(\gamma)} \right)^{\frac{1}{p}} \quad (11)$$

If it is known that for some (usually well-depolarized) state  $V = V^*$  one has  $m_\infty(V^*) = 1$  (but note that this can only ever be approximately true as  $m_\infty$  can only approach unity asymptotically) then the maximal conductance  $\bar{g}$  can be estimated from voltage clamp experiments from

$$\bar{g} = \frac{I_{max}(V^*)}{(V^* - V_{rev})F_p(\gamma(V^*))}. \quad (12)$$

Once  $\bar{g}$  is known then (11) can be used to find  $m_\infty(V_1)$  for various  $V_1$  because all remaining quantities,  $I_{max}$ ,  $(V_1 - V_{rev})$  and  $F_p(\gamma(V_1))$  are known.

In summary, the steps to find the activation function  $m_\infty(V)$  are:

- (a) From the time course of the current find the maximum current and its time of occurrence for a given  $V_1$
- (b) Estimate the time constants  $\tau_m(V_1)$  and  $\tau_h(V_1)$  and the value of  $p$ .
- (c) Hence find  $\gamma(V_1)$  and also  $F_p(\gamma(V_1))$ .
- (d) Using a suitably highly depolarized state  $V = V^*$  estimate  $\bar{g}$  according to (12).
- (e) Hence estimate  $m_\infty(V)$  at various  $V$  below  $V^*$ .
- (f) Find the best fitting Boltzmann curve passing through the values obtained.

However, the formulas (6)-(8) were derived on the assumption that  $h(V_1) = 1$  and this will usually be valid for  $V_c < V_1 < V^*$ , where  $V_c$  is below the half-activation potential  $V_a$ . This means that the half-activation function  $m_\infty(V)$  can be obtained accurately for  $V \geq V_a$ , and thus by symmetry for  $V < V_a$ . Another approach is as follows.

#### 4.2.2 $V^*$ is not known: least squares estimates

If  $V^*$  is not known or is uncertain, then least squares estimates can be made as follows. It is assumed that

$$m_\infty(V) = \frac{1}{1 + e^{-(V-V_a)/k_a}} \quad (13)$$

is the steady state activation function. Then one may estimate  $\bar{g}$ ,  $V_a$  and  $k_a$  by minimizing the sum of squares of the differences between experimentally obtained maxima of the current at various  $V_i$  and the values given by formula (8)

#### 4.2.3 Summary of methods A-D used to estimate the activation function

Here is given a brief description of the 4 methods employed to estimate the parameters of  $m_\infty(V)$  and  $\bar{g}$  given in Table 2.

##### Method A

Having estimated the values of the time constants  $\tau_m(V_i)$  and  $\tau_h(V_i)$  and the power  $p$  as described in the text, experimental maximum currents at various  $V_i$  are compared with those obtained from formula (8)

$$I_{max}(V_i) = \bar{g}(V_i - V_{rev})m_\infty^p(V_i)F_p(\gamma) \quad (14)$$

with  $\gamma$  evaluated at  $V_i$ . Thus the parameters  $\bar{g}$ ,  $V_a$  and  $k_a$  are estimated by least squares.

##### Method B

It is assumed that  $m_\infty(V^*) = 1$ , with  $V^* = -20$  mV in the present example, so that  $\bar{g}$  is given directly by Equation (12). Then  $m_\infty(V_i)$  can be obtained for

various  $V_i$  using Equation (11). A best fitting Boltzmann is then obtained for the various values of  $m_\infty(V_i)$ .

#### Method C

The experimental values of the maximum currents (over time)  $I_{i,max}(V_i)$  at each test voltage  $V_i$  are divided by  $V_i - V_{rev}$  to give corresponding conductances  $G_i(V_i)$ . The conductances  $G_i(V_i)$  are assumed (from Equation (8) without the correction factor) to be given by

$$G_i(V_i) = \bar{g}m_\infty^p(V_i). \quad (15)$$

With

$$m_\infty(V) = \frac{1}{1 + e^{-(V-V_a)/k_a}} \quad (16)$$

the parameters  $\bar{g}$ ,  $V_a$  and  $k_a$  (and possibly  $p$  if not already known) are estimated by least squares fitting of the experimental  $G_i$  values to the predicted ones, without any assumption on  $V^*$  (normalization).

#### Method D

The same procedure is carried out as in method C, but the  $G_i$  values are divided by the maximum value  $G_{max}$ , assumed to occur at  $V^*$  (-20 mV in the above), to give the normalized values

$$\tilde{G}_i = \frac{G_i}{G_{max}}. \quad (17)$$

Then since  $\tilde{G}_i(V^*) = 1$  there are only two parameters  $V_a$  and  $k_a$  to estimate with a best fitting Boltzmann curve. The maximal conductance  $\bar{g}$  can be obtained as

$$\bar{g} = \frac{I_{max}(V^*)}{V^* - V_{rev}}. \quad (18)$$

#### 4.2.4 No inactivation

If there is no inactivation in the course of the clamp experiment then the maximum current will be the asymptotic value

$$I_{max}(V_1) = \bar{g}(V_1 - V_{rev})m_\infty^p(V_1). \quad (19)$$

So, with  $V^*$  as above,  $\bar{g}$  is again given by (18), and it is straightforward to obtain the required activation function from the remaining  $I_{max}$  measurements.

#### 4.2.5 Inactivation experiments

Here steps are made from a number of relatively hyperpolarized states  $V_0$  to a fixed relatively depolarized state  $V_1$ . It is usually assumed that  $h_1 = 0$  and  $m_0 = 0$ , so that the current is approximately

$$I(t; V_0, V_1) = \bar{g}(V_1 - V_{rev})m_\infty^p(V_1)h_\infty(V_0)(1 - e^{-t/\tau_m})^p e^{-t/\tau_h}. \quad (20)$$

Here the time course of the current (but not its magnitude) is the same for all  $V_0$ .

The time of occurrence of the maximum  $t_{max}$  of  $I(t; V_0; V_1)$  is again given by (7) but the value of the maximum is now

$$I_{max}(V_0, V_1) = \bar{g}(V_1 - V_{rev})m_{\infty}^p(V_1)h_{\infty}(V_0)F_p(\gamma). \quad (21)$$

Assuming that  $\bar{g}$  has already been estimated and that  $V^*$  is such that  $m_{\infty}(V^*) = 1$ , then the inactivation function can be found at  $V_0$  from

$$h_{\infty}(V_0) = I_{max}(V_0, V^*)\bar{g}(V^* - V_{rev})F_p(\gamma(V^*)) \quad (22)$$

It can be seen that normalizing the currents by dividing by the maximum of the  $I_{max}$  gives a reasonable estimate of the steady state inactivation function.

## Acknowledgements

Support from the Max Planck Institute is appreciated (HCT). We appreciate useful correspondence with Professor John Huguenard (Stanford University) and Professor John Bekkers (Australian National University).

## References

- Aghajanian, G.K., 1985. Modulation of a transient outward current in serotonergic neurones by  $\alpha_1$ -adrenoceptors. *Nature* 315, 501-503.
- Bekkers, J.M., 2000. Properties of voltage-gated potassium currents in nucleated patches from large layer 5 cortical pyramidal neurons of the rat. *J Physiol* 525.3, 593-609.
- Belluzzi, O., Sacchi, O., 1988. The interactions between potassium and sodium currents in generating action potentials in the rat sympathetic neurone. *J Physiol* 397, 127-147.
- Burlhis, T.M., Aghajanian, G.K., 1987. Pacemaker potentials of serotonergic dorsal raphe neurons: contribution of a low-threshold  $\text{Ca}^{2+}$  conductance. *Synapse* 1, 582-588.
- Chen, Y., Yao, Y., Penington, N.J., 2002. Effect of pertussis toxin and *N*-ethylmaleimide on voltage-dependent and -independent calcium current modulation in serotonergic neurons. *Neuroscience* 111, 207-214.
- Connor, J.A., Stevens, C.F., 1971. Prediction of repetitive firing behaviour from voltage clamp data on an isolated neurone soma. *J Physiol* 213, 31-53.
- Destexhe, A., Neubig, M., Ulrich, D., Huguenard, J., 1998. Dendritic low-threshold calcium currents in thalamic relay cells. *J Neurosci* 18, 3574-3588.
- Destexhe, A., Rudolph, M., Fellous, J-M., Sejnowski, T.J., 2001. Fluctuating synaptic conductances recreate *in vivo*-like activity in neocortical neurons. *Neuroscience* 107, 13-24.

- Faber, G.M., Silva, J., Livshitz, L., Rudy, Y., 2007. Kinetic properties of the cardiac L-Type  $\text{Ca}^{2+}$  Channel and its role in myocyte electrophysiology: a theoretical investigation. *Biophys J* 92, 1522-1543.
- Gutman, G.A., Chandy, K.G., Grissmer, S., Lazdunski, M., Mckinnon, D., Pardo, L.A., Robertson, G.A., Rudy, B., Sanguinetti, M.C., Stühmer, W., Wang, X., 2005. International Union of Pharmacology. LIII. Nomenclature and molecular relationships of voltage-gated potassium channels. *Pharmacol Rev* 57, 473-508.
- Hamill, O.P., Marty, A., Neher, E., Sakmann, B., Sigworth, F.J., 1981. Improved patch-clamp techniques for high-resolution current recording from cells and cell-free membrane patches. *Pflügers Arch* 391, 85-100.
- Hodgkin, A.L., Huxley, A.F., 1952. A quantitative description of membrane current and its application to conduction and excitation in nerve. *J Physiol* 117, 500-544.
- Komendantov, A.O., Komendantova, O.G., Johnson, S.W., Canavier, C.C., 2004. A modeling study suggests complementary roles for GABA<sub>A</sub> and NMDA receptors and the SK channel in regulating the firing pattern in midbrain dopamine neurons. *J Neurophysiol* 91, 346-357.
- Koschak, A., Reimer, D., Walter, D. et al., 2003.  $\text{Ca}_v1.4\alpha_1$  subunits can form slowly inactivating dihydropyridine-sensitive L-type  $\text{Ca}^{2+}$  channels lacking  $\text{Ca}^{2+}$ -dependent inactivation. *J Neurosci* 23, 6041-6049.
- Kuznetsova, A.Y., Huertas, M.A., Kuznetsov, A.S., Paladini, C.A., Canavier, C.C., 2010. Regulation of firing frequency in a computational model of a midbrain dopaminergic neuron. *J Comp Neurosci* 28, 389-403.
- Liu, R.-J., van den Pol, A.N., Aghajanian, G.K., 2004. Hypocretins (orexins) regulate serotonin neurons in the dorsal raphe nucleus by excitatory direct and inhibitory indirect actions. *J Neurosci* 22, 9453-9464.
- Marcantoni, A., Vandael, D.H.F., Mahapatra, S., Carabelli, V., Sinnegger-Brauns, M.J., Striessnig, J., Carbone, E., 2010. Loss of  $\text{Ca}_v1.3$  channels reveals the critical role of L-type and BK channel coupling in pacemaking mouse adrenal chromaffin cells. *J Neurosci* 30, 491-504.
- McCormick, D.A., Huguenard, J.R., 1992. A model of the electrophysiological properties of thalamocortical relay neurons. *J Neurophysiol* 68, 1384-1400.
- Migliore, M., Cook, E.P., Jaffe, D.B., Turner, D.A., Johnston, D., 1995. Computer simulations of morphologically reconstructed CA3 hippocampal neurons. *J Neurophysiol* 73, 1157-1168.
- Miyazaki, K., Miyazaki, K.W., Doya, K., 2011. Activation of dorsal raphe serotonin neurons underlies waiting for delayed rewards. *J Neurosci* 31, 469-479.
- Penington, N.J., Fox, A.P., 1995. Toxin-insensitive Ca current in dorsal raphe neurons. *J Neurosci* 15, 5719-5726.
- Penington, N.J., Kelly, J.S., Fox, A.P., 1991. A study of the mechanism of  $\text{Ca}^{2+}$  current inhibition produced by serotonin in rat dorsal raphe neurons. *J Neurosci* 11, 3594-3609.

- Penington, N.J., Kelly, J.S., Fox, A.P., 1992. Action potential waveforms reveal simultaneous changes in  $I_{Ca}$  and  $I_K$  produced by 5-HT in rat dorsal raphe neurons. *Proc R Soc Lond. B* 248, 171-179.
- Penington, N.J., Fox, A.P., (1995) Toxin-insensitive Ca Current in dorsal raphe neurons. *J Neurosci* 15, 5719-5725.
- Poirazi, P., Brannon, T., Mel, B.W., 2003. Arithmetic of subthreshold synaptic summation in a model CA1 pyramidal cell. *Neuron* 37, 977-987.
- Putzier, I., Kullmann, P.H.M., Horn, J.P., Levitan, E.S., 2009.  $Ca_v1.3$  channel voltage dependence, not  $Ca^{2+}$  selectivity, drives pacemaker activity and amplifies bursts in nigral dopamine neurons. *J Neurosci* 29, 15414-15419.
- Rhodes, P.A., Llinás, R., 2005. A model of thalamocortical relay cells. *J Physiol* 565, 765-781.
- Segal, M., 1985. A potent transient outward current regulates excitability of dorsal raphe neurons. *Brain Res* 359, 347-350.
- Steinbusch, H.W., Nieuwenhuys, R., Verhofstad, A.A., Van der Kooy, D., 1981. The nucleus raphe dorsalis of the rat and its projection upon the caudatoputamen. A combined cytoarchitectonic, immunohistochemical and retrograde transport study. *J Physiol (Paris)* 77, 157-174.
- Traub, R.D., Wong, R.K.S., Miles, R., Michelson, H., 1991. A model of a CA3 hippocampal pyramidal neuron incorporating voltage-clamp data on intrinsic conductances. *J Neurophysiol* 66, 635-650.
- Traub, R.D., Buhl, E.H., Gloveli, T., Whittington, M.A., 2003. Fast rhythmic bursting can be induced in layer 2/3 cortical neurons by enhancing persistent  $Na^+$  conductance or by blocking BK channels. *J Neurophysiol* 89, 909-921.
- Williams, G.S.B., Smith, G.D., Sobie, E.A., Jafri, M.S., 2010. Models of cardiac excitation-contraction coupling in ventricular myocytes. *Math Biosci* 226, 1-15.
- Xu, J., Clancy, C.E., 2008. Ionic mechanisms of endogenous bursting in CA3 hippocampal pyramidal neurons: a model study. *PLoS ONE* 3, e2056.
- Yao, Y., Bergold, P., Penington, N.J., 2010. Acute  $Ca^{2+}$ -dependent desensitization of 5-HT<sub>1A</sub> receptors is mediated by activation of protein kinase A (PKA) in rat serotonergic neurons. *Neuroscience* 169, 87-97.
- Yamamoto, M., Steinbusch, H.W., Jessell, T.M., 1981. Differentiated properties of identified serotonin neurons in dissociated cultures of embryonic rat brain stem. *J Cell Biol* 91,142-152.
- Yu, Y., Shu, Y., McCormick, D.A., 2008. Cortical action potential backpropagation explains spike threshold variability and rapid-onset kinetics. *J Neurosci* 28, 7260-7272.